[CANCER RESEARCH 61, 4490–4496, June 1, 2001]

Epidermal Growth Factor Receptor-targeted Immunophotodiagnosis and Photoimmunotherapy of Oral Precancer *in Vivo*[1]

Nikolaos S. Soukos, Michael R. Hamblin, Suzanne Keel, Richard L. Fabian, Thomas F. Deutsch, and Tayyaba Hasan[2]

Wellman Laboratories of Photomedicine, Departments of Dermatology [N. S. S., M. R. H., T. F. D., T. H.] and Pathology [S. K.], Massachusetts General Hospital, and Department of Otolaryngology/Head and Neck Surgery, Massachusetts Eye and Ear Infirmary [R. L. F.], Harvard Medical School, Boston, Massachusetts 02114

ABSTRACT

Immunophotodiagnosis uses a fluorescence-labeled monoclonal antibody (MAb) that recognizes a tumor-associated antigen to image the fluorescence emitted from the fluorophore-bound MAb that has localized in the tissue. It may be used to diagnose malignant or precancerous lesions, to delineate the margins for tumor resection, or as a feedback mechanism to assess response to treatment. In oral precancer, the epidermal growth factor receptor (EGFR) is overexpressed and could be used as a marker for early detection or as a target for therapy. The goal of this study was to test an anti-EGFR MAb (C225) coupled to either the near-infrared fluorescent dye *N,N′*-di-carboxypentyl-indodicarbocyanine-5,5′-disulfonic acid for detection or a photochemically active dye (chlorin$_{e6}$) for therapy of early premalignancy in the hamster cheek pouch carcinogenesis model. Fluorescence levels in the carcinogen-treated tissue correlated with the histological stage of the lesions when the C225-*N,N′*-di-carboxypentyl-indodicarbocyanine-5,5′-disulfonic acid conjugate was used but did not do so with the irrelevant conjugates. Discrete areas of clinically normal mucosa with high fluorescence (hot spots) were subsequently shown by histology to contain dysplastic areas. The best contrast between normal and carcinogen-treated cheek pouches was found at 4–8 days after injection. To test the potential of immunophotodiagnosis as a feedback modality for therapeutic intervention, experiments were conducted with the same MAb conjugated to chlorin$_{e6}$ followed by illumination to reduce expression of the EGFR by a photodynamic effect. Subsequent immunophotodiagnosis showed that this treatment led to a significant reduction in fluorescence in the carcinogen-treated cheek pouch compared with nonilluminated areas. This difference between illuminated and dark areas was not seen in the normal cheek pouch. Taken together, the results demonstrate the potential for development of immunophotodiagnosis as a diagnostic tool and as a method of monitoring response to therapy and that the EGFR may be an appropriate target in head and neck cancer.

INTRODUCTION

Oral precancer includes all of the stages on the route to oral malignancy (1). It may represent a clinically unrecognizable preinvasive state arising against the background of clinically normal mucosa or a clinically recognizable premalignant lesion, either leukoplakia (white patch) or erythroplakia (red patch; Ref. 2). If oral precancer is not detected and treated early, then moderately advanced oral cancer at the time of diagnosis has a poor prognosis (2). A simple, safe, and highly acceptable diagnostic test should enable the clinician to detect the earliest signs of SCC[3] during a routine screening. In addition, effective treatment of early oral precancer should be noninvasive and should selectively destroy premalignant cells, leaving surrounding tissues undamaged.

Head and neck cancers including oral cancer and precancer (3–5) as well as other types of epithelial malignancies (6–9) overexpress the EGFR, a 170-kDa glycoprotein with an intrinsic tyrosine-specific protein kinase activity stimulated upon EGF binding (10). EGFR was found to be up-regulated in human normal oral epithelium adjacent to tumor and remained elevated throughout the progress from hyperplasia to dysplasia, and the expression was dramatically increased when dysplasia progressed to SCC (11). Significant EGFR overexpression was also detected in the chemically induced malignant transformation leading to carcinoma in the hamster cheek pouch model (12). These findings suggest that the overexpression of EGFR might be used as a marker for early diagnosis and treatment of oral precancer (13).

Anti-EGFR MAbs labeled with radioisotopes have been used for diagnosis of several types of cancers (14, 15). These MAbs have also been used with therapeutic intent and have been shown to lead to inhibition of tumor growth when administered alone (16) and to produce enhancement of the antitumor activity of chemotherapy (15, 17). MAbs coupled with fluorescent dyes, such as fluorescein (18, 19) and indocyanine (20), have also been used for diagnostic purposes. On the other hand, covalent conjugation of PSs, such as chlorins, to MAbs has been proposed to enhance the selectivity of PDT *in vitro* (21, 22) and *in vivo* (23, 24). Anti-EGFR MAb conjugated to the PS benzoporphyrin derivative was shown to improve the selectivity and efficacy of PDT for SCC in the hamster cheek pouch model (25).

Targeting the EGFR with antibody-delivered photoactive molecules may serve as a two-armed feedback-controlled approach: the PS together with illumination may destroy the EGFR and cause the premalignant lesion to regress, and the fluorescent dye may allow the progress of the treatment to be monitored. As a first step toward realizing this goal, the present study had two immediate aims: (*a*) to determine whether the i.v. injection of a conjugate between an anti-EGFR MAb (C225) and the fluorescent dye indocyanine Cy5.5 could deliver sufficient amounts of the fluorophore into clinically unrecognizable early premalignant lesions in the hamster cheek pouch carcinogenesis model to make them detectable by fluorescence imaging; and (*b*) to test the photodynamic effect of a conjugate between C225 and the PS c$_{e6}$, followed by illumination, in animals with early lesions and to examine the effect of the treatment on tissue levels of EGFR by the immunophotodiagnosis procedure after subsequent administration of C225-Cy5.5.

MATERIALS AND METHODS

Animal Model. Syrian golden hamster cheek pouch carcinogenesis closely replicates events involved in the development of premalignancy in human oral cancer (26). Male Syrian golden hamsters (*Mesocricetus auratus*; 80–100 g) were obtained from the Charles River Animal Research Facility (Boston, MA) at 4–6 weeks of age. Animals were housed four to a cage at room temperature with wood chips for bedding and a 12-h light/dark cycle. Water and laboratory chow were given *ad libitum*. All procedures received approval from the Subcommittee on Research Animal Care of Massachusetts General Hospital before the start of the study.

Epithelial changes characteristic of the progress to early premalignancy

Received 11/13/00; accepted 3/29/01.

The costs of publication of this article were defrayed in part by the payment of page charges. This article must therefore be hereby marked *advertisement* in accordance with 18 U.S.C. Section 1734 solely to indicate this fact.

[1] Supported by Department of Energy Grant DE-FG02-91-ER61228 (to N. S. S.), Department of Defense Medical Free Electron Laser Program Grant N 00014-94-1-0927 (to M. R. H. and T. F. D.), and NIH Grant R01 AR40352 (to T. H.).

[2] To whom requests for reprints should be addressed, at Department of Dermatology, Massachusetts General Hospital, 50 Blossom Street WEL224, Boston, MA 02114-2698. Phone: (617) 726-6996; Fax: (617) 726-3192; E-mail: hasan@helix.mgh.harvard.edu.

[3] The abbreviations used are: SCC, squamous cell carcinoma; c$_{e6}$, chlorin$_{e6}$; Cy5.5, *N,N′*-di-carboxypentyl-indodicarbocyanine-5,5′-disulfonic acid; DMBA, 7,12-dimethylbenz(*a*)anthracene; EGFR, epidermal growth factor receptor; MAb, monoclonal antibody; NHS, *N*-hydroxysuccinimide; PIT, photoimmunotherapy; PS, photosensitizer; PDT, photodynamic therapy; HCPC, hamster cheek pouch carcinoma; CCD, charge-coupled device.

were induced by thrice weekly (Monday, Wednesday, and Friday) topical application using a Q-tip of 50–100 μl of a 0.5% solution of DMBA (Sigma Chemical Co., St. Louis, MO) in mineral oil on the right buccal pouch mucosa for 6 weeks. Initial studies also used 12 weeks of application of DMBA to give papillary tumors measuring 4–6 mm in diameter. Injection of drugs into the subclavian vein and immunophotodiagnosis and PIT studies were performed under i.p. anesthesia with a mixture of ketamine, xylazine, and atropine (80–100, 5–10, and 0.04 mg/kg, respectively). The hamsters were euthanized in a CO_2 chamber. At the time of euthanasia, animals weighed between 180 and 220 g. After euthanasia, the cheek pouches were excised along with the underlying connective tissue and musculature, and routine histology (H&E staining) was performed.

Chemicals. The MAb C225 was kindly provided by ImClone Systems, Inc. (Somerville, NJ). Cy5.5 FluoroLink Dye (bifunctional NHS ester in sealed foil packets) was obtained from Amersham Life Science (Arlington Heights, IL). c_{e6} was obtained from Porphyrin Products (Logan, UT). BSA and mouse IgG were obtained from Sigma Chemical Co.

Preparation of Conjugates. Cy5.5 conjugates were prepared by dissolving 2 mg of protein (C225, BSA, or mouse IgG) in 2 ml of 0.1 M sodium bicarbonate buffer (pH 9.3). The content of one Cy5.5 foil pack was dissolved in sodium bicarbonate buffer (200 μl) and added to the protein solution with shaking. The mixture was incubated in the dark at room temperature for 3 h, and then it was dialyzed three times against 5 liters of 0.01 M phosphate buffer (pH 7.4) to remove any unbound dye.

c_{e6}-NHS ester was prepared as a solution in DMSO as described previously (27). C225 (2 mg) was dissolved in 2 ml of sodium bicarbonate buffer, and DMSO solution containing NHS ester of 200 μg of c_{e6} equivalent was added with stirring. This is a 25-fold molar excess of c_{e6} to IgG. After 24 h of incubation in the dark at room temperature, the preparation was exhaustively dialyzed (at least three times) against 5 liters of 0.01 M phosphate buffer (pH 7.4). After characterization by spectrophotometry, Cy5.5 and c_{e6} conjugates were stored at 4°C in the presence of 10% (v/v) horse serum (to prevent aggregation) and 15 mM sodium azide.

Cell Lines. The human epidermoid SCC line A431 was obtained from the American Type Culture Collection (Manassas, VA). The HCPC-1 cell line was developed from the culture of an experimentally induced epidermoid carcinoma of the buccal pouch (28) and was a generous gift of Dr. Joel Schwartz (Department of Oral Pathology, Harvard School of Dental Medicine, Boston, MA). Cells were grown in DMEM with high glucose (Life Technologies, Inc., Grand Island, NY) supplemented with 10% FCS (Life Technologies, Inc.), 100 units/ml penicillin G, and 100 μg/ml streptomycin (Sigma Chemical Co.). Medium was changed every 2–3 days, and cells were passaged weekly using trypsin-EDTA (Life Technologies, Inc.). All cells were maintained in 10-cm-diameter Petri dishes with 12-ml of growth medium and kept at 37°C in a humidified 95% air:5% CO_2 atmosphere.

***In Vitro* Immunoreactivity of the C225-Cy5.5 Conjugate with Tumor Cells.** HCPC-1 and A431 cells were grown in P35 dishes containing 5 ml of growth medium and a 22-mm square glass coverslip until they were 60–70% confluent. The C225-Cy5.5, BSA-Cy5.5, or mouse IgG-Cy5.5 conjugates were added at a final concentration of 0.1 μg Cy5.5 equivalent/ml in serum-containing medium for 3 h at 37°C. The coverslips were then washed three times with PBS, put on histological slides in PBS, and examined with an epi-illumination fluorescence microscope (Axiophot; Zeiss, Oberkochen, Germany) equipped with a cooled CCD camera (CE200; Photometrics, Tucson, AZ). Images were obtained using excitation light provided by a mercury vapor lamp and a 670 ± 5 nm bandpass filter, and the emission was collected with a long-pass filter at 700 nm.

Fluorescence Imaging. Imaging was conducted with a Pulnix room temperature CCD camera (model TM 745; Pulnix America, Inc., Sunnyvale, CA) with the anesthetized hamster placed on a movable stage approximately 50 cm below the camera. To avoid any reflectance, the cheek pouches were put on a black cloth covering a polystyrene platform and firmly attached to it using pins with a diameter of 100 μm. Each hamster was marked on both cheek pouches with Indian ink to give the maximum size rectangle possible within the exposed surface. The CCD camera was interfaced to an integration system (Pulnix) allowing integration of the signal for up to 1 s. The cheek pouches were illuminated with 670 nm light from an argon-ion (Innova 100; Coherent, Inc., Palo Alto, CA) pumped dye laser (CR-599; Coherent, Inc.) at a power density of 15 mW/cm^2 (450 mW total power) measured with a power meter (model 200; Coherent, Inc.). The light was delivered to the imaging plane through a 1-mm-diameter fiber optic and expanded to give homogenous spot of 5-cm in diameter using a 4× objective lens with numerical aperture of 0.1.

Fluorescence images were captured with an integration time of 1 s and with two filters placed before the camera lens. The first filter was a 700 nm bandpass interference filter with a bandwidth of 10 nm full width half maximum (Andover Corp., Salem, NH), and the second was a long-pass absorption filter with a 50% cutoff wavelength at 690 nm (Andover Corp.) and was used to remove fluorescence induced in the first filter. Excitation at 670 nm gave the optimum balance of power from the laser and excitation light rejection by the filters and allowed fluorescence images to be captured at a low level of background light. A white-light image of each specimen was first captured to inspect the cheek pouch. Fluorescence images from the CCD camera were captured using an 8-bit/pixel frame grabber (model DT 2867; Data Translation, Marlboro, MA) controlled by the computer program Global Lab Image (v2.20; Data Translation). The laser beam rested on each cheek pouch for 5 s to acquire each image; therefore, because the tissue was illuminated with 15 mW/cm^2, it receives a fluence of 0.075 J/cm^2 of energy. Each hamster was imaged before injection and on days 1, 2, 4, 6, and 8 after injection.

Each image series was analyzed by image analysis software (Global Lab Image v2.20). The India ink markings were visible on the fluorescence images as dark spots due to the absence of fluorescence. Two predefined regions were delineated for each hamster: (*a*) one covers the entire area between the India ink markings; and (*b*) the other covers the hot spot (if any) and was measured from the nearest two markings to be reproduced at each time point. The image analysis software gave the mean pixel intensity on a 256 gray-scale and the SD for each area. Measurements of average pixel intensity on the black background cloth surrounding the cheek pouch were taken for background correction. Each measurement of tissue fluorescence had the background measurement subtracted from it, yielding what is referred to as the absolute fluorescence.

Immunophotodetection of Premalignant Lesions. Before fluorescence imaging was undertaken, the cheek pouch mucosae were inspected and photographed to evaluate the lesions. Initial fluorescence imaging studies used three hamsters that had developed gross papillary tumors after 12 weeks of painting of the cheek pouch. These animals were injected with 670 μg of C225-Cy5.5 conjugate (the average Cy5.5:MAb ratio was 2.1:1) corresponding to 12 μg of Cy5.5 and imaged 2 days later. For imaging of oral premalignant lesions, 27 hamsters bearing lesions produced by painting the right cheek pouches for 6 weeks were studied. Nine hamsters were injected with C225-Cy5.5 as described above. Six control animals received 610 μg of irrelevant mouse IgG-Cy5.5 conjugate (the average Cy5.5:IgG ratio was 2.3:1) also corresponding to 12 μg of Cy5.5. Another group of six control animals was injected with 390 μg of BSA-Cy5.5 conjugate (the average Cy5.5:BSA ratio was 1.6:1) corresponding to 12 μg of Cy5.5 to distinguish between EGFR binding and increased vascular permeability. In all cases, the overall dose of Cy5.5 injected was 100 μg/kg body weight.

At the end of the fluorescence imaging studies, biopsies (approximately 25 mm^2) were obtained to correlate the fluorescent signals with the histologically determined stage of the lesions. In the case of cheek pouches that showed a fluorescent hot spot, one biopsy was taken from the hot spot, and another was taken from a part of the cheek pouch distant from the hot spot. Tissue samples were immediately placed in 10% formalin followed by routine processing for paraffin embedding and histological study. Sections were stained with H&E and examined by light microscopy.

PIT *in Vivo*. A pilot study investigated the photodynamic effect of the C225-c_{e6} conjugate on EGFR expression in early premalignant lesions (6 weeks of DMBA treatment) of the hamster cheek pouch of 11 hamsters. Before injection of C225-c_{e6}, the visible area of each cheek pouch (DMBA-treated and normal tissue) was divided in two equal parts using India ink, and the outer part of each cheek pouch to be exposed to light was marked, whereas the inner part was protected from light by a black cloth. Animals were injected with 3.38 mg of C225-c_{e6} conjugate (the average c_{e6}:MAb ratio was 4.8:1, corresponding to 65 μg of c_{e6}), and 666 nm light was applied 2 days later (total fluence = 100 J/cm^2 delivered at a power density of 50 mW/cm^2). The effectiveness of the treatment was assessed by immunophotodiagnosis by injecting the C225-Cy5.5 conjugate as described above at 5 days posttreatment. Fluorescence imaging was performed 3 days after injection of the C225-Cy5.5 conjugate.

Statistics. SDs of ratios of two means were calculated by the use of addition in quadrature (29). The difference between two means was tested for significance by a two-sided Student's *t* test, assuming equal or unequal variances as appropriate. Means of ratios were tested to see whether they were significantly >1 by one-sided Student's *t* test.

RESULTS

Preparation and Characterization of Conjugates. The absorption spectra of the C225-Cy5.5 and BSA-Cy5.5 conjugates together with free Cy5.5 are shown in Fig. 1*A*. The conjugates have a distinct peak at 284 nm due to the protein absorbance by IgG and BSA, and the peak due to the Cy5.5 is at 675 nm for all conjugates. The number of dyes/protein molecule can be calculated assuming extinction coefficients of 2.5×10^5 M^{-1} cm^{-1} for Cy5.5 at 675 nm, 1.7×10^5 M^{-1} cm^{-1} for IgG (corrected for absorbance of Cy5.5 at 284 nm), and 1.2×10^5 M^{-1} cm^{-1} for BSA at 284 nm (likewise corrected for absorbance of Cy5.5). The C225-Cy5.5 conjugate had 2.1 molecules of Cy5.5 attached to each IgG, whereas BSA had 1.6 molecules/protein molecule.

Because the effectiveness of the c_{e6} conjugates in the destruction of premalignant tissue may depend on the amount of PS able to be delivered to the lesion, it was desirable to have as high a loading of c_{e6} as possible, consistent with the MAb still retaining its immunoreactivity. In the present case, the loading of the c_{e6} conjugates was limited by their tendency to aggregate when the ratio increased beyond 5 molecules c_{e6}/IgG. The absorption spectra of C225-c_{e6} and free c_{e6} are shown in Fig. 1*B*. The conjugate has a distinct absorbance at 284 nm due to the protein in the IgG, the intensity of the Soret band is somewhat reduced, and the long wavelength Q band is red shifted to 666 nm as opposed to 654 nm. It can be calculated assuming extinction coefficients of 1.5×10^5 lmol^{-1} cm^{-1} for c_{e6} at the Soret band and 2.4×10^5 lmol^{-1} cm^{-1} for IgG at 280 nm. The C225-c_{e6} conjugate had a loading of 4.8 molecules c_{e6}/IgG.

Fluorescence Localization in Living Cells. The fluorescence images of A431 and HCPC-1 cells that had been incubated with the C225-Cy5.5 conjugate at a final concentration of 0.1 μg of Cy5.5 equivalent in serum-containing medium for 3 h at 37°C are shown in Fig. 2, *a* and *c*, along with the corresponding bright-field images (Fig. 2, *b* and *d*). The conjugate showed a strong affinity for A431 cells, which was expected because these cells have a high number of EGFRs (30). In addition, a significant fluorescence was seen with HCPC-1 cells, indicating the suitability of the conjugate for targeting the DMBA tumor model. Neither cell line showed fluorescence after incubation with BSA-Cy5.5 or mouse IgG-Cy5.5 conjugates (data not shown).

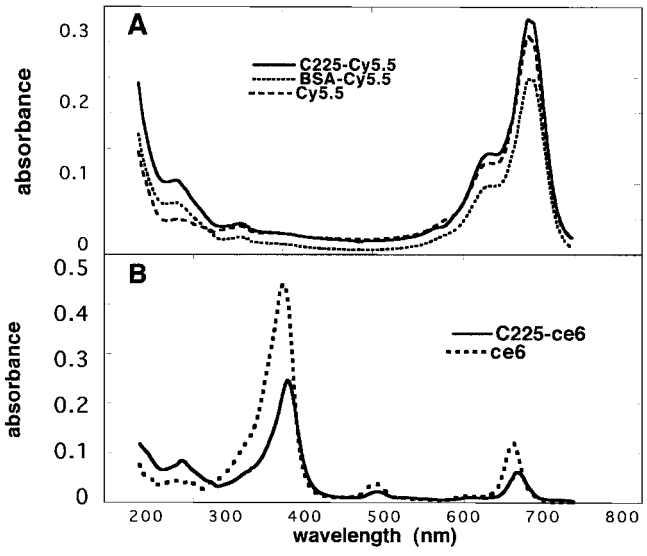

Fig. 1. UV-visible absorption spectra in 0.1 M NaOH/0.1% SDS. *A*, C225-Cy5.5, mouse IgG-Cy5.5, and BSA-Cy5.5 conjugates and unconjugated Cy5.5; *B*, C225-c_{e6} and c_{e6}.

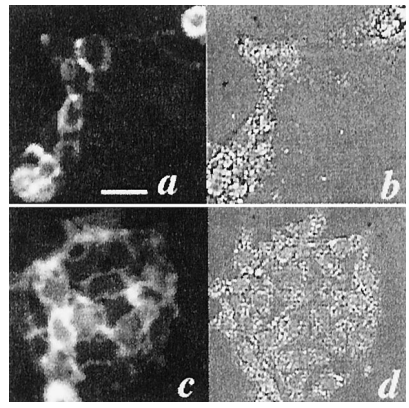

Fig. 2. Fluorescence localization of C225-Cy5.5 with A431 and HCPC-1 cells. Cells were incubated with the conjugate at a final concentration of 0.1 μg of Cy5.5 equivalent in serum-containing medium for 3 h at 37°C (670 nm, bandpass filter excitation; 700 nm, long-pass filter emission). A431 cells with the C225-Cy5.5 conjugate: fluorescence image, *a*; bright-field image, *b*. HCPC-1 cells with the C225-Cy5.5 conjugate: fluorescence image, *c*; bright-field image, *d*. *Bar*, 50 μm.

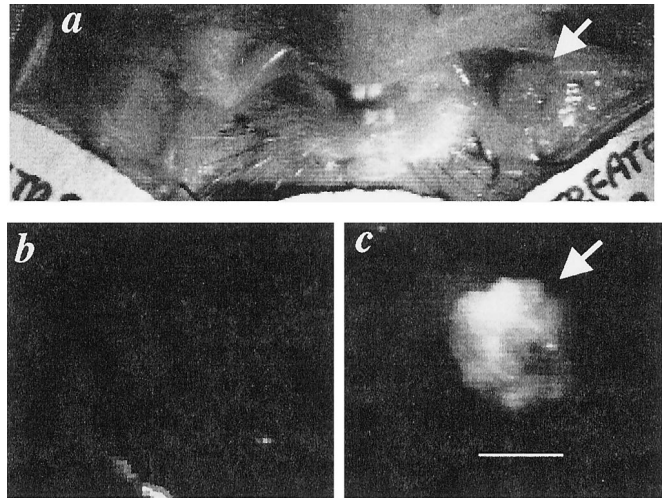

Fig. 3. Fluorescence image of hamster with gross papillary tumor obtained after 12 weeks of painting of the cheek pouch with DBMA. Hamsters were injected with 670 μg of C225-Cy5.5 and imaged 2 days later. *a*, white-light image of both cheek pouches. *b*, fluorescence image of normal cheek pouch. *c*, fluorescence image of carcinogen-treated cheek pouch with papillary tumor (*arrow*); *bar*, 5 mm.

Immunophotodiagnosis of Oral Precancer *in Vivo*. Initially, immunophotodiagnosis was performed on three animals with gross papillary tumors obtained after painting of cheek pouches for 12 weeks. A representative image from an animal with a papillary tumor measuring 5 mm in diameter is shown in Fig. 3. The normal cheek pouch has no visible fluorescence, whereas the tumor-bearing pouch has a clearly delineated tumor in the fluorescence image. Note that the fluorescence from the tumor is not completely uniform, and this nonuniformity does not appear to be due to the illumination conditions, suggesting that the expression of the EGFR is heterogeneous, or the perfusion is nonuniform.

To examine the use of immunophotodiagnosis in animals with hyperplastic or dysplastic lesions, we used hamsters that had been

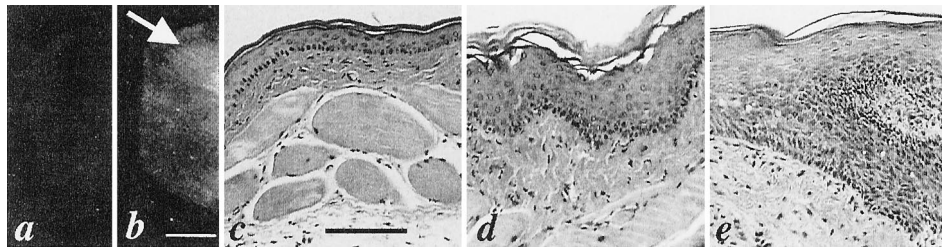

Fig. 4. Fluorescence images of normal (*a*) and DMBA-treated (*b*) cheek pouches in hamster 6 at 6 days after the injection of the C225-Cy5.5 conjugate. *Bar*, 5 mm. A fluorescence hot spot (area of increased fluorescence) can be seen within the DMBA-treated cheek pouch (*arrow*). H&E histology shows (*c*) normal mucosal epithelium for the DMBA-untreated cheek pouch (*bar*, 100 μm), (*d*) mild dysplasia for the DMBA-treated cheek pouch, and (*e*) moderate dysplasia for the hot spot.

painted with DMBA for an average of 6 weeks. Animals were injected with C225-Cy5.5 or the control dye conjugates (mouse IgG-Cy5.5 or BSA-Cy5.5) and imaged on days 1, 2, 4, 6, and 8 after injection. A representative pair of images captured from the DMBA-treated and control cheek pouch in hamster 6 at 6 days after injection of C225-Cy5.5 is shown in Fig. 4. The mean values of the ratios of fluorescence of DMBA-treated cheek pouches:normal cheek pouches from groups of hamsters injected with the EGFR-targeted C225-Cy5.5 and nontargeted conjugates (mouse IgG-Cy5.5 and BSA-Cy5.5) are shown in Table 1. The ratios from the C225-Cy5.5 group were significantly greater than 1 for all time points except 1 day after injection. None of the control groups had mean ratios that were statistically >1. The histological diagnoses of the animals in the control groups were similar, with about 50% of the hamsters in each group showing focal dysplasia or hyperplasia.

Five of nine animals in the C225-Cy5.5 group showed a distinct and circumscribed area of increased fluorescence (termed a hot spot) within the overall increased fluorescence of the clinically normal DMBA-treated cheek pouch (see Fig. 4). The fluorescence values from these hot spots were calculated separately, and the resulting mean absolute values are plotted together with the overall (whole cheek pouch) mean absolute fluorescence values against time after injection in Fig. 5. The fluorescence intensities from the whole cheek pouches were highest 1 day after the injection of the C225-Cy5.5 conjugate (2 days after injection in the case of the hot spots) and then dropped in an apparent exponential decay.

Table 2 shows the correlation between the fluorescence ratios (DMBA-treated cheek pouches:normal cheek pouches) and the histological diagnosis of biopsies taken from whole (clinically normal) cheek pouches and from fluorescent hot spots located within cheek pouches of five hamsters. As can be seen, four of five of the hot spots showed evidence of dysplasia in the hot spot tissue, whereas only one (hamster 6) showed dysplasia outside of the hot spot. The remaining hot spot (hamster 3, which had the lowest fluorescence ratio) showed only hyperkeratosis and an inflammatory infiltrate.

PIT Studies. These experiments were performed to test the hypothesis that C225 could selectively deliver a PS to the EGFR in these early premalignant lesions and that after illumination, the resultant photodynamic effect would reduce the expression of the EGFR. Furthermore, immunophotodiagnosis could be used as a feedback tool for PIT, and the tissue fluorescence level may act as a surrogate marker for efficacy. We hypothesized that the effects of PIT on EGFR levels could be demonstrated by comparison of fluorescence images produced by C225-Cy5.5 in the cheek pouches at 5 days after treatment. A total of 11 hamsters had one cheek pouch painted with carcinogen for 6 weeks, and then each animal was injected with C225-c_{e6}. Three days later, part of each cheek pouch (carcinogen-treated and normal tissue) was illuminated with red light (100 J/cm^2). Five days later, animals were injected with C225-Cy5.5 as described previously, and after another 3 days, fluorescence images were obtained. Four mean fluorescence values from the areas of cheek pouches were obtained and are shown in Table 3. As expected, there was a highly significant difference between the mean fluorescence values of the non-light-exposed areas of the normal and DMBA-treated cheek pouches (110 ± 21 *versus* 160 ± 29, $P < 0.0005$). The mean fluorescence values of the light-treated and non-light-treated areas of the normal cheek pouches were almost the same (112 ± 22 *versus* 110 ± 21). When the light-exposed DBMA-treated areas were compared with the non-light-exposed DMBA-treated areas, there was a significant reduction in fluorescence (124.2 ± 26 *versus* 160 ± 29, $P < 0.01$), and interestingly, there was no significant difference between the light-exposed DMBA-treated areas and either the light-exposed or the dark areas of the normal cheek pouches. This latter result suggests that the overexpression of the EGFR found after DMBA treatment had been reduced to background levels after PIT. After completion of the fluorescence imaging, the animals were sacrificed, and the cheek pouches were subjected to histological examination. All 11 hamsters had hyperkeratosis and focal hyperplasia in the DMBA-treated pouches, and 2 animals also had focal dysplasia. The light-exposed areas of both normal and DMBA-treated pouches also revealed a submucosal edema and inflammatory infiltrate.

DISCUSSION

The results obtained in this study show that the use of anti-EGFR MAb-targeted photoactive dyes may serve as a feedback-controlled optical diagnosis and therapy procedure for oral premalignant lesions.

The indocyanine dyes, such as the one used in the present study, have advantages over fluorescein, a dye that has been used for diagnostic purposes in both animal models (18) and humans (19). The longer wavelength emission penetrates tissue significantly better, and they have high fluorescence quantum yields and good solubility (31). More specifically, the indocyanine dye Cy5.5 emits a near-infrared fluorescence at 702 nm after excitation at 675 nm and has an extremely high molar absorption coefficient. These properties of Cy5.5

Table 1 *Ratios of fluorescence intensities from DMBA-treated and normal cheek pouches*[a]

	Day 1	Day 2	Day 4	Day 6	Day 8
C225-Cy5.5 ($n = 9$)	1.17 ± 0.25	1.19 ± 0.16	1.56 ± 0.51	1.54 ± 0.46	1.85 ± 0.44
	n.s.[b]	$P < 0.005$	$P < 0.005$	$P < 0.005$	$P < 0.0005$
mIgG-Cy5.5 ($n = 6$)	1.01 ± 0.12	1.05 ± 0.12	1.07 ± 0.06	0.96 ± 0.09	
BSA-Cy5.5 ($n = 6$)	0.95 ± 0.18	0.98 ± 0.36	0.90 ± 0.15	0.99 ± 0.01	

[a] Ratios of mean fluorescence values (DMBA-treated cheek pouch:normal cheek pouch) from groups of hamsters at different time intervals after the injection of the specified conjugate. Values are means and SD calculated in quadrature.
[b] n.s., not significant.

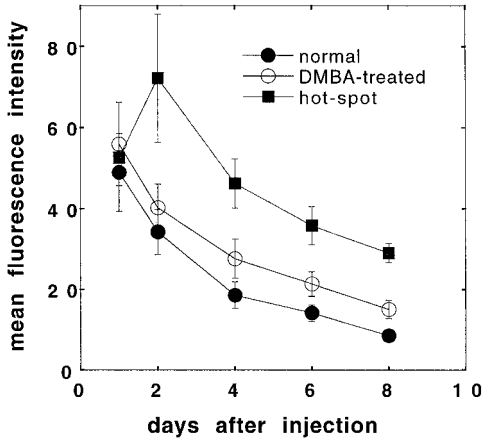

Fig. 5. Time course of mean absolute fluorescence values in the DMBA-treated *versus* DMBA-untreated cheek pouches after injection of the C225-Cy5.5 conjugate. Values from normal and DMBA-treated cheek pouches are from nine hamsters, whereas values of hot spot fluorescence are from five hamsters. Values are expressed as means ± SE.

should lead to increased sensitivity of detection of premalignant lesions because fluorescence from molecules localized deeper into tissue can be detected. Furthermore, background autofluorescence is minimized because the endogenous fluorophores present in tissue do not absorb at 675 nm (the excitation wavelength of Cy5.5). The C225-Cy5.5 conjugate used in this study, with a dye:MAb molar ratio of 2:1, was efficient in detection of oral premalignant lesions. Folli *et al.* (19) have also shown the suitability of an indocyanine-MAb conjugate with the same molar ratio for the detection of tumors in nude mice using the marker dye Cy5 with excitation and emission wavelengths of 640 and 667 nm, respectively. This indocyanine-MAb conjugate showed almost the same circulating half-life and tumor localization capacity as the unconjugated MAb (19).

The injection of the conjugate was well tolerated by the animals and produced a sufficiently bright fluorescence signal to allow quantitative imaging. At early time points (up to 24 h), the C225-Cy5.5 conjugate was distributed primarily within and near the vasculature. The same observations were also obtained using the BSA-Cy5.5 conjugate. Thus, fluorescence measurements in both DMBA-treated and normal cheek pouches showed average fluorescence intensity values with high SDs because fluorescence was obtained mainly from the cheek pouch capillaries. The microvascular changes observed in the cheek pouch capillary network 6 weeks after the first application of DMBA were similar to those observed by Lurie *et al.* (32) in the same model. Control cheek pouches contained a plexus of capillaries with uniform diameters that were connected to larger vessels, but the diameters of capillaries in DMBA-treated cheek pouches were larger than those of control cheek pouches. At 2 days postinjection, the fluorescence signal originated mainly from extravascular dye within the tissue. Although in a number of studies, immunophotodetection of malignant tumors was possible in animals and humans 24 h after the injection of either fluorescein (18, 19, 33)- or indocyanine-labeled (20, 31, 34) MAbs, we did not observe any striking difference in fluorescence images obtained from control and premalignant tissue 24 h after the injection of the conjugate. There was some contrast between normal and premalignant tissue 2 days after the injection of the conjugate, but the best contrast was obtained at 4–8 days. The increase in contrast after 2 days is probably due to the relatively slow removal of nonspecifically bound MAb conjugate that has escaped from the vasculature into the tissue.

It has been reported that certain types of tumor vasculature have a dramatically increased permeability to macromolecules (35, 36). This increased permeability has been reported (37) to account for some of the tumor-localizing ability of MAb conjugates. In the present study, a BSA-Cy5.5 conjugate was used to test the possibility of a nonspecific macromolecule giving increased fluorescence in the lesions due to preferential extravasation. Hyperpermeability of blood vessels in premalignant lesions may not be the case here because these lesions were very early. Our fluorescence imaging system could distinguish between premalignant lesions and normal mucosa, and in addition, dysplastic areas could be detected as fluorescent hot spots. Histopathological examination of excised tissue from these areas dem-

Table 2 *Ratios of fluorescence intensities from DMBA-treated and normal cheek pouches in individual animals injected with C225-Cy5.5 Ratios of fluorescence values (DMBA-treated cheek pouch:normal cheek pouch) from individual hamsters at different time intervals after the injection of the C225-Cy5.5 conjugate correlated with the histologically determined stage of the premalignant lesion. Values are means and SD calculated in quadrature.*

A. Ratio of mean fluorescence intensities (DMBA-treated:normal pouches)						
Animal no.	Day 1	Day 2	Day 4	Day 6	Day 8	Microscopic diagnosis from H&E-stained fixed slides
1	1.2	1.13	1.53	1.16		Hyperkeratosis
2	1.06	1.05	1.09	0.92		Hyperkeratosis
3[a]	0.94	1.05	1.08	1.23	1.33	Hyperkeratosis
4	1.23	1.16	1.23	1.02	1.49	Hyperkeratosis
5	0.94	1.07	1.07	1.9	2.3	Hyperkeratosis
6[a]	1.06	1.13	2	2.18	1.56	Dysplasia[b]
7[a]	1.76	1.48	2.09	1.74	2.23	Hyperkeratosis, hyperplasia
8[a]	1.17	1.24	2.45	1.99		Hyperkeratosis
9[a]	1.17	1.43	1.48	1.68	2.2	Hyperkeratosis
B. Fluorescence ratios from hot spot (hot spot:normal cheek pouch)						Microscopic diagnosis from hot spot
3		1.55	1.57	1.87	2.02	Hyperkeratosis, strong inflammatory infiltrate
6			2.3	3.31		Dysplasia[c]
7		2.35	2.68	2.4	3.38	Dysplasia[d]
8	1.63	1.84	3.54	2.66		Dysplasia[a]
9	1.45	1.86	1.63	1.87	2.48	Dysplasia[f]
Mean ± SD	1.54 ± 0.13	1.9 ± 0.33	2.34 ± 0.81	2.42 ± 0.6	2.63 ± 0.69	
*P*s for mean > 1		<0.0005	<0.001	<0.001	<0.005	

[a] Areas with DMBA-treated cheeck pouches that showed an increased fluorescence signal (hot spots) were found.
[b] Hyperkeratosis, hyperplasia, and drop-shaped rete processes.
[c] Hyperkeratosis, irregular epithelial downgrowth, loss of basal cell polarity, increased nuclear:cytoplasmic ratio, and a small number of abnormal mitoses.
[d] Hyperkeratosis, irregular epithelial downgrowth, and loss of basal cell polarity.
[e] Hyperkeratosis, hyperplasia, nuclear hyperchromatism, and strong inflammatory infiltrate.
[f] Hyperkeratosis, hyperplasia, irregular epithelial downgrowth, deep cell keratinization, and enlarged prickle cells.

Table 3 *Mean absolute fluorescence values from illuminated (light) and nonilluminated (dark), carcinogen-treated (DMBA) and normal cheek pouches treated with PIT followed by immunophotodiagnosis*

Values are means and SD.

$n = 11$ hamsters	Normal/dark	Normal/light	DMBA/dark	DMBA/light
Mean absolute fluorescence	110.1 + 20.8	112.7 + 21.9	160.0 + 25.1	124.2 + 26.4
P vs. Normal/dark		n.s.[a]	<0.0005	n.s.
P vs. Normal/light			<0.0005	n.s.
P vs. DBMA/dark				<0.01

[a] n.s., not significant.

onstrated the presence of dysplasia. This suggests that different levels of the C225-Cy5.5 conjugate were retained in lesions at different stages of carcinogenesis, reflecting increased numbers of EGFRs in dysplastic lesions. Other workers have used PSs designed for PDT to carry out fluorescence diagnosis of premalignant lesions in the hamster cheek pouch. These PSs include Photofrin (38, 39) and 2-[1-hexyloxyethyl]-2-devinyl pyropheophorbide-a (40), and the free dye fluorescein has also been used (41). However, Andrejevic Blant *et al.* (42) failed to detect any increased fluorescence in premalignant lesions using the PS benzoporphyrin derivative or tetra(*m*-hydroxyphenyl)chlorin.

The apparent significance of the EGFR in human cancer has prompted several efforts to use it as a therapeutic target. Several murine MAbs that bind and block the binding of ligand to EGFRs were able to inhibit the proliferation of a variety of human cancer cell lines in culture and in xenograft tumor models (43). A link between EGFR signaling and angiogenesis has recently been identified (44). It has been reported that systemic administration of MAb C225 inhibited the growth and metastasis of human transitional cell carcinoma established in the bladder wall of athymic nude mice in part by inhibition of angiogenesis (45). The use of conjugates between an anti-EGFR MAb and a PS to target photodynamic treatment to the EGFR is an approach with many advantages. It combines the specificity of the MAb with the spatial confinement of light delivery in which damage will be limited to the irradiated volume of tissue and should reduce side effects. In addition, these photoimmunoconjugates do not necessarily need to be internalized to impose their effect. Photodestruction of EGFRs should result in a more lasting reduction of growth signals in the nucleus than merely blocking the binding of EGF. The ultimate goal of this treatment is the inhibition of cellular proliferation, and additional studies should follow the progression of the animals' lesions over time. The photodynamic effects of a conjugate between an anti-EGFR MAb and the PS benzoporphyrin derivative have been studied on SCC in the hamster cheek pouch model (25). The conjugate was effective for PIT, producing an 80% rate of complete response.

In conclusion, our results suggest that immunophotodiagnosis using C225-Cy5.5 may have potential both as a diagnostic modality for oral precancer and as a surrogate marker for disease progression. The use of a near-infrared emitting fluorophore as a label may be an alternative to using radioisotopes, with consequent increased patient safety. To extend the analogy with radioisotopes, the principle of using an anti-EGFR MAb to deliver photoactive molecules applies equally well to therapeutic PSs as to fluorophores, and furthermore, immunophotodiagnosis can be used to assess response. Additional studies should correlate the histology and long-term tissue response of dysplastic lesions, with the immunofluorescence signals obtained in both treated and control lesions. Mechanistic studies to identify the site at which the actual damage is inflicted and to investigate the repair of the signaling pathway should also be conducted.

ACKNOWLEDGMENTS

We thank Michael P. Bamberg, Jaimie L. Miller, and Bart Johnson for technical assistance; ImClone Systems, Inc. for the gift of MAb C225; and Coherent, Inc. for the loan of the argon-pumped dye laser. We also thank Dr. Brian W. Pogue for useful advice and suggestions concerning the setup of the fluorescence imaging system.

REFERENCES

1. Speight, P. M., and Morgan, P. R. The natural history and pathology of oral cancer and precancer. Community Dent. Health, *10* (Suppl. 1)*:* 31–41, 1993.
2. Scully, C. Clinical diagnostic methods for the detection of premalignant and early malignant oral lesions. Community Dent. Health, *10* (Suppl. 1)*:* 43–52, 1993.
3. Eisbruch, A., Blick, M., Lee, J. S., Sacks, P. G., and Gutterman, J. Analysis of the epidermal growth factor receptor gene in fresh human head and neck tumors. Cancer Res., *47:* 3603–3605, 1987.
4. Shirasuna, K., Hayashido, Y., Sugiyama, M., Yoshioka, H., and Matsuya, T. Immunohistochemical localization of epidermal growth factor (EGF) and EGF receptor in human oral mucosa and its malignancy. Virchows Archiv. A Pathol. Anat. Histol., *418:* 349–353, 1991.
5. Ke, L. D., Adler-Storthz, K., Clayman, G. L., Yung, A. W., and Chen, Z. Differential expression of epidermal growth factor receptor in human head and neck cancers. Head Neck, *20:* 320–327, 1998.
6. Rusch, V., Baselga, J., Cordon-Cardo, C., Orazem, J., Zaman, M., Hoda, S., McIntosh, J., Kurie, J., and Dmitrovsky, E. Differential expression of the epidermal growth factor receptor and its ligands in primary non-small cell lung cancers and adjacent benign lung. Cancer Res., *53:* 2379–2385, 1993.
7. Harris, A. L., Nicholson, S., Sainsbury, J. R., Neal, D., Smith, K., Farndon, J. R., and Wright, C. Epidermal growth factor receptor: a marker of early relapse in breast cancer and tumor stage progression in bladder cancer; interactions with *neu*. *In:* M. Furth and M. Greaves (eds.), The Molecular Diagnosis of Human Cancer, pp. 353–357. Cold Spring Harbor, NY: Cold Spring Harbor Laboratory, 1989.
8. Neal, D. E., Marsh, C., Bennett, M. K., Abel, P. D., Hall, R. R., Sainsbury, J. R., and Harris, A. L. Epidermal-growth-factor receptors in human bladder cancer: comparison of invasive and superficial tumours. Lancet, *1:* 366–368, 1985.
9. Humphrey, P. A., Wong, A. J., Vogelstein, B., Friedman, H. S., Werner, M. H., Bigner, D. D., and Bigner, S. H. Amplification and expression of the epidermal growth factor receptor gene in human glioma xenografts. Cancer Res., *48:* 2231–2238, 1988.
10. Carpenter, G. Receptors for epidermal growth factor and other polypeptide mitogens. Annu. Rev. Biochem., *56:* 881–914, 1987.
11. Shin, D. M., Ro, J. Y., Hong, W. K., and Hittelman, W. N. Dysregulation of epidermal growth factor receptor expression in premalignant lesions during head and neck tumorigenesis. Cancer Res., *54:* 3153–3159, 1994.
12. Shin, D. M., Gimenez, I. B., Lee, J. S., Nishioka, K., Wargovich, M. J., Thacher, S., Lotan, R., Slaga, T. J., and Hong, W. K. Expression of epidermal growth factor receptor, polyamine levels, ornithine decarboxylase activity, micronuclei, and transglutaminase I in a 7,12-dimethylbenz(*a*)anthracene-induced hamster buccal pouch carcinogenesis model. Cancer Res., *50:* 2505–2510, 1990.
13. Todd, R., and Wong, D. T. Epidermal growth factor receptor (EGFR) biology and human oral cancer. Histol. Histopathol., *14:* 491–500, 1999.
14. Goldenberg, A., Masui, H., Divgi, C., Kamrath, H., Pentlow, K., and Mendelsohn, J. Imaging of human tumor xenografts with an indium-111-labeled anti-epidermal growth factor receptor monoclonal antibody. J. Natl. Cancer Inst. (Bethesda), *81:* 1616–1625, 1989.
15. Divgi, C. R., Welt, S., Kris, M., Real, F. X., Yeh, S. D., Gralla, R., Merchant, B., Schweighart, S., Unger, M., Larson, S. M., *et al.* Phase I and imaging trial of indium 111-labeled anti-epidermal growth factor receptor monoclonal antibody 225 in patients with squamous cell lung carcinoma. J. Natl. Cancer Inst. (Bethesda), *83:* 97–104, 1991.
16. Fan, Z., Masui, H., Altas, I., and Mendelsohn, J. Blockade of epidermal growth factor receptor function by bivalent and monovalent fragments of 225 anti-epidermal growth factor receptor monoclonal antibodies. Cancer Res., *53:* 4322–4328, 1993.
17. Baselga, J., Pfister, D., Cooper, M. R., Cohen, R., Burtness, B., Bos, M., D'Andrea, G., Seidman, A., Norton, L., Gunnett, K., Falcey, J., Anderson, V., Waksal, H., and Mendelsohn, J. Phase I studies of anti-epidermal growth factor receptor chimeric antibody C225 alone and in combination with cisplatin. J. Clin. Oncol., *18:* 904–914, 2000.
18. Pelegrin, A., Folli, S., Buchegger, F., Mach, J. P., Wagnieres, G., and van den Bergh, H. Antibody-fluorescein conjugates for photoimmunodiagnosis of human colon carcinoma in nude mice. Cancer (Phila.), *67:* 2529–2537, 1991.
19. Folli, S., Wagnieres, G., Pelegrin, A., Calmes, J. M., Braichotte, D., Buchegger, F., Chalandon, Y., Hardman, N., Heusser, C., and Givel, J. C. Immunophotodiagnosis of colon carcinomas in patients injected with fluoresceinated chimeric antibodies against carcinoembryonic antigen. Proc. Natl. Acad. Sci. USA, *89:* 7973–7977, 1992.
20. Folli, S., Westermann, P., Braichotte, D., Pelegrin, A., Wagnieres, G., van den Bergh, H., and Mach, J. P. Antibody-indocyanin conjugates for immunophotodetection of human squamous cell carcinoma in nude mice. Cancer Res., *54:* 2643–2649, 1994.
21. Hamblin, M. R., Miller, J. L., and Hasan, T. Effect of charge on the interaction of site-specific photoimmunoconjugates with human ovarian cancer cells. Cancer Res., *56:* 5205–5210, 1996.
22. Goff, B. A., Bamberg, M., and Hasan, T. Photoimmunotherapy of human ovarian carcinoma cells *ex vivo*. Cancer Res., *51:* 4762–4767, 1991.

23. Duska, L. R., Hamblin, M. R., Bamberg, M. P., and Hasan, T. Biodistribution of charged $F(ab')_2$ photoimmunoconjugates in a xenograft model of ovarian cancer. Br. J. Cancer, *75:* 837–844, 1997.
24. Molpus, K. L., Hamblin, M. R., Rizvi, I., and Hasan, T. Intraperitoneal photoimmunotherapy of ovarian carcinoma xenografts in nude mice using charged photoimmunoconjugates. Gynecol. Oncol., *76:* 397–404, 2000.
25. Hemming, A., Davis, N., Dubois, B., Quenville, N., and Finley, R. Photodynamic therapy of squamous cell carcinoma. An evaluation of a new photosensitizing agent, benzoporphyrin derivative, and new photoimmunoconjugate. Surg. Oncol., *2:* 187–196, 1993.
26. Shklar, G., Eisenberg, E., and Flynn, E. Immunoenhancing agents and experimental leukoplakia and carcinoma of the hamster buccal pouch. Prog. Exp. Tumor Res., *24:* 269–282, 1979.
27. Soukos, N. S., Hamblin, M. R., and Hasan, T. The effect of charge on cellular uptake and phototoxicity of polylysine chlorin($_{e6}$) conjugates. Photochem. Photobiol., *65:* 723–729, 1997.
28. Odukoya, O., Schwartz, J., Weichselbaum, R., and Shklar, G. An epidermoid carcinoma cell line derived from hamster 7,12-dimethylbenz[*a*]anthracene-induced buccal pouch tumors. J. Natl. Cancer Inst. (Bethesda), *71:* 1253–1264, 1983.
29. Taylor, J. R. (ed.). An Introduction to Error Analysis, p. 57. Mill Valley, CA: University Science Books, 1982.
30. Kawamoto, T., Sato, J. D., Le, A., Polikoff, J., Sato, G. H., and Mendelsohn, J. Growth stimulation of A431 cells by epidermal growth factor: identification of high-affinity receptors for epidermal growth factor by an antireceptor monoclonal antibody. Proc. Natl. Acad. Sci. USA, *80:* 1337–1341, 1983.
31. Ballou, B., Fisher, G. W., Hakala, T. R., and Farkas, D. L. Tumor detection and visualization using cyanine fluorochrome-labeled antibodies. Biotechnol. Prog., *13:* 649–658, 1997.
32. Lurie, A. G., Tatematsu, M., Nakatsuka, T., Rippey, R. M., and Ito, N. Anatomical and functional vascular changes in hamster cheek pouch during carcinogenesis induced by 7,12-dimethylbenz(*a*)anthracene. Cancer Res., *43:* 5986–5994, 1983.
33. Tatsuta, M., Iishi, H., Ichii, M., Baba, M., Yamamoto, R., Okuda, S., and Kikuchi, K. Diagnosis of gastric cancers with fluorescein-labeled monoclonal antibodies to carcinoembryonic antigen. Lasers Surg. Med., *9:* 422–426, 1989.
34. Ballou, B., Fisher, G. W., Waggoner, A. S., Farkas, D. L., Reiland, J. M., Jaffe, R., Mujumdar, R. B., Mujumdar, S. R., and Hakala, T. R. Tumor labeling *in vivo* using cyanine-conjugated monoclonal antibodies. Cancer Immunol. Immunother., *41:* 257–263, 1995.
35. Dvorak, H. F., Nagy, J. A., Dvorak, J. T., and Dvorak, A. M. Identification and characterization of the blood vessels of solid tumors that are leaky to circulating macromolecules. Am. J. Pathol., *133:* 95–109, 1988.
36. Yuan, F., Leunig, M., Huang, S. K., Berk, D. A., Papahadjopoulos, D., and Jain, R. K. Microvascular permeability and interstitial penetration of sterically stabilized (stealth) liposomes in a human tumor xenograft. Cancer Res., *54:* 3352–3356, 1994.
37. Dvorak, H. F., Nagy, J. A., and Dvorak, A. M. Structure of solid tumors and their vasculature: implications for therapy with monoclonal antibodies. Cancer Cells (Cold Spring Harbor), *3:* 77–85, 1991.
38. Crean, D. H., Liebow, C., Penetrante, R. B., and Mang, T. S. Evaluation of porfimer sodium fluorescence for measuring tissue transformation. Cancer (Phila.), *72:* 3068–3077, 1993.
39. Mang, T. S., McGinnis, C., Liebow, C., Nseyo, U. O., Crean, D. H., and Dougherty, T. J. Fluorescence detection of tumors. Early diagnosis of microscopic lesions in preclinical studies. Cancer (Phila.), *71:* 269–276, 1993.
40. Furukawa, K., Yamamoto, H., Crean, D. H., Kato, H., and Mang, T. S. Localization and treatment of transformed tissues using the photodynamic sensitizer 2-[1-hexyloxyethyl]-2-devinyl pyropheophorbide-a. Lasers Surg. Med., *18:* 157–166, 1996.
41. Lazarev, V. V., Roth, R. A., Kazakevich, Y., and Hang, J. Detection of premalignant oral lesions in hamsters with an endoscopic fluorescence imaging system. Cancer (Phila.), *85:* 1421–1429, 1999.
42. Andrejevic Blant, S., Ballini, J. P., van den Bergh, H., Fontolliet, C., Wagnieres, G., and Monnier, P. Time-dependent biodistribution of tetra(*m*-hydroxyphenyl)chlorin and benzoporphyrin derivative monoacid ring A in the hamster model: comparative fluorescence microscopy study. Photochem. Photobiol., *71:* 333–340, 2000.
43. Mendelsohn, J., and Baselga, J. Antibodies to growth factors and receptors. *In:* A. P. J. DeVita, S. Hellman, and S. A. Rosenberg (eds.), Biologic Therapy of Cancer, 2nd ed., pp. 607–623. Philadelphia: J. B. Lippincott Co., 1995.
44. Petit, A. M., Rak, J., Hung, M. C., Rockwell, P., Goldstein, N., Fendly, B., and Kerbel, R. S. Neutralizing antibodies against epidermal growth factor and ErbB-2/neu receptor tyrosine kinases down-regulate vascular endothelial growth factor production by tumor cells *in vitro* and *in vivo*: angiogenic implications for signal transduction therapy of solid tumors. Am. J. Pathol., *151:* 1523–1530, 1997.
45. Perrotte, P., Matsumoto, T., Inoue, K., Kuniyasu, H., Eve, B. Y., Hicklin, D. J., Radinsky, R., and Dinney, C. P. Anti-epidermal growth factor receptor antibody C225 inhibits angiogenesis in human transitional cell carcinoma growing orthotopically in nude mice. Clin. Cancer Res., *5:* 257–265, 1999.